PROCEEDINGS OF ECOS 2023 - THE 36TH INTERNATIONAL CONFERENCE ON
EFFICIENCY, COST, OPTIMIZATION, SIMULATION AND ENVIRONMENTAL IMPACT OF ENERGY SYSTEMS
25-30 JUNE, 2023, LAS PALMAS DE GRAN CANARIA, SPAIN

Thermo-economic optimization of a Carnot Battery under transient conditions

Márcio Santos[a], Jorge André[b], Ricardo Mendes[c] and José B. Ribeiro[d]

[a] University of Coimbra, ADAI-LAETA, Coimbra, Portugal, marcio.santos@dem.uc.pt,
[b] University of Coimbra, ADAI-LAETA, Coimbra, Portugal, jorge.andre@dem.uc.pt,
[c] University of Coimbra, ADAI-LAETA, Coimbra, Portugal, ricardo.mendes@dem.uc.pt,
[d] University of Coimbra, ADAI-LAETA, Coimbra, Portugal, jose.baranda@dem.uc.pt

Abstract:

With the efforts to decarbonize the energy sector comes a growing demand of electricity, most of which is to be supplied by renewable generation in a carbon-neutral future. To balance the variability inherent to most renewable energy sources, some form of energy storage is required. In this work, a short review of current systems is made with a particular focus on Carnot Batteries, whose operating characteristics, long life and low environmental footprint make them competitive for daily energy storage. A transient model was developed to simulate the full operation of a Carnot Battery composed of a Vapour Compression Heat Pump and Organic Rankine Cycles in conjunction with sensible thermal storage. The key performance parameters were identified, and a Pareto optimization was carried out by balancing costs and performance across 25 configurations of storage temperature spread and heat exchanger pinch point. It was concluded that the wider storage spreads and higher pinch points lead to lower costs as they decrease the size of the water tank and the heat exchangers, and to lower efficiencies as unfavourable temperature gradients are created for the heat pump and heat engine. A Pareto front was identified, consisting of 10 configurations that were able to either optimize one criterion, or balance of two or more criteria, and conclusions were drawn as to the applicability of each configuration.

Keywords:

Carnot Battery, Thermal Energy Storage, Electric Energy Storage, Heat Pump, Organic Rankine Cycle

1. Introduction

According to the IPCC (Intergovernmental Panel for Climate Change), human-induced warming has already reached approximately 1ºC, in 2017. If all human emissions were to be immediately reduced to zero, it's estimated that the total rise in temperature in the time scale of a century would fall under 1.5ºC, in relation to pre-industrial levels. The Paris Agreement has set a goal to limit this global temperature rise to 2ºC, and preferably to keep it under 1.5ºC, as this would substantially reduce the effects of climate change in relation to a future in which no action is taken.

According to the RNC2050 (Roteiro para a Neutralidade Carbónica – Roadmap for Carbon Neutrality), a long-term plan for achieving net-zero emissions by 2050, the biggest drivers for decarbonization of the energy sector are the use of renewables, increased energy efficiency (which translates into reduced demand from sources), electrification, and new energy vectors such as hydrogen and other synthetic fuels. It states also that the inherent variability of most widespread renewable sources (namely wind and solar PV) creates problems of dispatchability and energy security. The document states that strong grid interconnection with the European Union, smart energy management, and increased usage of Energy Storage Systems (ESS) are key to solving these issues. This notion is supported by the scientific community, as current papers highlight the necessity for energy storage, often in conjunction with an interconnected and smart grid, to effectively manage the supply variability (on many time scales) resulting from large-scale renewable integration.

1.1. The Challenges of decarbonization in terms of energy storage

The need for inertia in our energy systems is clear – to mitigate variability in supply. However, while most issues caused by integration of Variable Renewable Energy (VRE) sources fall into this category, the features that characterize each problem vary in terms of power requirement, storage duration, discharge time, response time, and other technical characteristics.

The load Shifting and Seasonal Storage is the most important application of energy storage in the context of decarbonization. Because of the largely uncontrollable nature of VREs, supply of electric energy will rarely

https://doi.org/10.52202/069564-0196

match demand, so, in these cases, we often require storage systems to shift the supply to more favourable periods of time, to satisfy demand and prevent curtailing.

The needed storage duration will vary depending on the characteristics of the generation source, but it should fit roughly in the time scale of its natural variation; this can range from a few hours – the case for solar variation [1] – to days, weeks or even months – the typical long-term variation in wind speeds [2], [1].

Power requirements must also match the generation source, in the order of 10-100 MW for grid scale applications, with lower values for localized/consumer-scale situations. Maximum response times must be in the scale of minutes, and the capacity should be sufficient to absorb excess power and satisfy demand. For large scale applications with seasonal storage, it may reach values in the order of 100-1000 MWh [2]. At a very small-time scale, fluctuations in supply and demand can affect the properties of electric currents, such as voltage and frequency [2]. To maintain the power quality of the supplied energy, storage systems are often used. For these applications, storage duration and capacity may be limited, however, power and response time are critical parameters, as power (in the order of kW to several MW, depending on the scale of consumption) is to be processed almost instantaneously, in the order of milliseconds.

The Transmission and Distribution Management is extremely important. With increasing loads being placed on electric grids, bottlenecks may appear in periods of peak consumption. Alongside other measures, such as economic incentives for shifting consumption, storage systems may be used to absorb excess loads and delay costly investments into power grids. The storage duration required should fit the variations in demand (several hours). Power and capacity requirements depend on the scale of the application but are like those of grid-scale load-shifting. Response times of up to a few minutes should be sufficient.

Another major feature of ESS is the Backup Power. At the consumer scale, energy storage may be desired to maintain an uninterrupted power supply in case of an outage. In this case, power requirements should match the consumption load (from a few kW to tens of MW), and storage capacity and duration should match the expected outage period (usually up to a few hours, with enough capacity to satisfy power requirements over this period – up to the order of 10 MWh). Response time is a critical parameter as the grid power must be replaced immediately – a response in the order of milliseconds is ideal.

Lastly, to effectively replace fossil fuels in the transportation industry, the storage medium to be used must have high specific energies and energy densities, along with a quick response time. Power-To-Fuel technologies that produce fuels compatible with current fossil-based systems are a good solution for this sector [1].

1.2. Classification of Existing Technologies

Energy may be stored in various forms, the most common being chemical potential, magnetic fields, electric fields, pressurized gas, gravitational potential, thermal energy, and synthetic fuels, as showed in Table 1 [1], [2]. In the literature, the classification of storage systems varies slightly from author to author, as the mechanisms employed by storage systems, as well as the perspectives from which we classify them, are diverse.

Table 1. *Classifications of ESS*

Stored Energy	Storage Mechanism	Examples
Electric	Electric and magnetic fields	Supercapacitors, SMES
Electrochemical	Reversible chemical reactions	Conventional Batteries, Flow Batteries, High-Temperature Batteries, Metal-Air Batteries
Mechanical	Gas pressure, gravitational potential, kinetic energy	CAES, PHS, Flywheel
Thermal	Heat capacity of a material, latent heat of phase change, endothermal and exothermal reactions	TES (Sensible, Latent, Thermochemical)
Chemical	Production of synthetic fuels	P2G, P2L

Pumped Hydro Storage (PHS), exploits the change in elevation between reservoirs of water in order to store energy in the form of gravitational potential. In charge mode, water is moved to a high elevation, increasing its potential energy, and in discharge mode this energy is converted into kinetic energy as the water flows back to the lower reservoir, passing through a turbine which generates electricity. PHS has a good degree of maturity and commercial exploitation [1], [3], and is suitable for high power and high energy applications. It has low energy costs and a relatively high efficiency; however, it comes with the downsides of high environmental impact, and geographical restrictions. Additionally, this technology is becoming increasingly difficult to exploit, as in most developed countries the potential for new installations is nearly exhausted [3], [4].

Compressed Air Energy Storage (CAES) is a system which stores energy in the form of gas pressure. In the charging process, air is compressed and sent into an underground reservoir, and in the discharge process this pressurized air is expanded in a gas turbine to generate electricity. These systems benefit from a very low

environmental impact (if fossil fuel use is avoided), and excellent power and storage capacities. However, they suffer from geographical limitations, as they most often require an underground cavern for storage.

Electrochemical batteries store energy in the form of a reversible chemical reaction – in the discharge process, a redox reaction generates an electric current between the two electrodes. For charging, the reaction is reversed, absorbing electric current. Due to the speed of the reactions, the response time of these batteries is nearly instantaneous, making them adequate for applications requiring some agility, such as power quality and managing quick changes in renewable generation; however, this kind of battery generally suffers from environmental issues, high costs, and limited cycle life. In the realm of conventional batteries, the most commonly used are lead-acid, lithium-ion, nickel-cadmium and nickel-metal hydride. Other less common types of batteries are flow batteries and high-temperature batteries.

Other types include: Flywheel Energy Storage, that is one of the simplest forms of storage where storage takes the form of kinetic energy of a rotating mass; Supercapacitors that are an upgrade of regular capacitors, which store energy by accumulation of positive and negative charges on either side of a dielectric; and Superconducting Magnetic Energy Storage (SMES) systems that store energy in the form of a magnetic field, induced by a dynamic electric field passed through a coil.

Finally, Thermal Energy Storage systems store energy in the heat capacity of a solid or liquid material (Sensible Heat Storage), the latent heat of a phase change (Latent Heat Storage) or in a reversible thermochemical reaction (Thermochemical Storage). These systems can also vary by the method through which the storage medium is charged. Concentrated Solar Power (CSP) plants, if coupled with thermal storage, use solar radiation to heat a storage medium, which can then discharge to a heat engine for electricity production [13]. Another possibility is Wind-powered Thermal Energy System (WTES), in which wind power is converted directly to heat, which is stored in a TES and later used to power a heat engine [13]. The thermal storage may also be charged using electricity, in which case the whole system may be designated a Carnot Battery, and if a heat pump is used to charge the system it is designated a Pumped Thermal Electricity Storage (PTES), so long as the heat is used to produce electricity in the discharge phase. The Carnot Battery presents several advantages that make it competitive with other forms of ESS, mainly in terms of environmental impact, flexibility and efficiency, and so it will be the focus of this work.

2. Carnot Batteries

Carnot Batteries work by establishing a thermal gradient between a high temperature (HT) reservoir and a low temperature (LT) reservoir. Electric energy is used to charge the system by forcing heat flow against the natural gradient, thus storing thermal exergy. In the discharge phase, the heat flows from the hot environment to the cold one, and this flow is used to produce work in a heat engine. According to O. Dumont et al. [3], a Carnot Battery (CB) is defined as an EES technology where there is always an electric input, and an electric output. A thermal input may be used to improve the performance of the CB; however, its primary purpose remains the storage of electric energy. Similarly, the battery may output useful thermal energy, but the electric output must be comparable with the electric input. In practice, the reservoirs may be physical ones, such as water tanks or solid materials, or their role may be taken up by the environment (for example, the ambient air). Similarly, electric heat pumps or resistance heaters may be used for charging, and any heat engine (Rankine, Brayton, others) or even a thermoelectric generator may be used for discharging.

Carnot Batteries offer roundtrip efficiencies (ε_{rt}) in a wide range depending on their boundary conditions [3], [5–7], low energy costs [1][3], and high lifetimes [1][3]. These systems are mostly competitive for electricity storage on the scale of several hours, in situations that demand low Power/Capacity ratios, with values of 1 kW /4 kWh and lower. They have a very low environmental impact, and no dependence on geographical conditions [1], making them a suitable competitor to PHS and CAES, whose geographical constraints pose a considerable limit to their exploitability on a large scale. For local, small-scale implementations, Carnot Batteries may also present an adequate replacement for chemical batteries, which are often expensive and environmentally unsafe. Additionally, an important advantage of Carnot Batteries is the ability to integrate additional thermal reservoirs (such as industrial waste heat), which act as additional exergy sources [3]. This thermal integration increases the ε_{rt} of the system, potentially to values greater than unity (>100%), by decreasing the work input or increasing the work output. In Table 2 a brief summary is given of the technical characteristics of some different Carnot battery technologies.

Table 2. Technical summary of Carnot Battery technologies (adapted from [3]).

Cycle	Brayton Cycle	Electrical heater and Rankine Cycle	Heat Pump and Rankine Cycle
Power [MW]	Up to 100	Up to 100	Up to 10*
Energy [MWh]	Up to 400	Up to 400	Up to 40*
Temp [°C]	[-70:1000]	Up to 750	Up to 150
Compactness [kW/m^3]	25	~4	[0.05–1.72]

https://doi.org/10.52202/069564-0196

Compactness [kWh/m3]	200	~36	[0.2–207]
Self-discharge	medium	Very low	[30–73]
ε_{rt} [%]	[60-70]	[12-55]	[70-150]**
Price [$/kW]	[395-875]	~376	[272–468]
Price [$/kWh]	[55–198]	~94	[68–117]
Estimated TRL	5	9	7
Typical fluids	Argon, Air	Water	R1233zd(E), CO_2, NH_3, water

* Possible to extend by association in series ** Thermally integrated

If a heat pump is used to charge the thermal storage, the system is designated Pumped Thermal Electrical Storage. These systems may use Brayton heat pumps (HP) with Brayton heat engines (HE), Vapour Compression Heat Pumps (VCHP) in conjunction with Rankine Cycles (RC), or Brayton heat pumps with Rankine Cycles [4]. The presence of a heat pump for the charge cycle is advantageous if the Coefficient of Performance (COP) is higher than one, as the roundtrip efficiency of a PTES is generally the product of the COP with the HE efficiency (if thermal storage efficiency is not considered). The use of a heat pump brings advantages in terms of thermal integration, as it can increase the performance of the heat pump and/or the heat engine. This thermal integration allows an increase in efficiency without complex modifications to the thermodynamic cycles and makes the PTES more flexible, as it may now receive two inputs (electric and thermal) instead of just one – in this sense, Thermally Integrated PTES (TI-PTES) may be seen as a hybrid energy storage and waste heat power plant.

Brayton PTES is usually comprised of a Brayton heat pump, based on the inverse Brayton cycle, and a Brayton heat engine, typically working between two sensible reservoirs [3]. The typical layout contains two thermal reservoirs and four machines (two compressors and two expanders), however in a reversible system this number could reduce to two. In a Brayton cycle, the working gas is compressed, heated and expanded, and then cooled before the next compression. As the work produced by expansion is greater than the work used in compression, the expander drives the compressor with a net positive work output (as with any heat engine, the driving force is a temperature gradient between the two reservoirs) – this is the cycle followed in the discharge process. For charging, the inverse process occurs – the gas is heated and compressed, drawing heat from the LT reservoir, and then cooled, storing heat in the HT reservoir, followed by expansion [3].

HP/RC systems combine Vapour Compression Heat Pumps with Rankine Cycles, where the VCHP charges the reservoirs with thermal exergy, and the Rankine Cycle produces work by harnessing the temperature difference between HT and LT reservoirs. By comparison with Brayton systems, Rankine-based PTES offers the advantages of high energy density and low temperature operation – these features allow for more compact storage, lower self-discharge, and potentially more efficient integration of waste heat. One of the advantages of HP/ORC systems is the use of commercially available equipment (pumps, compressors, expanders, heat exchangers, valves), which facilitates their construction [3], [4], [8]. The schematic configuration for HP and ORC systems and the corresponding T-s diagrams are shown in Figure 1.

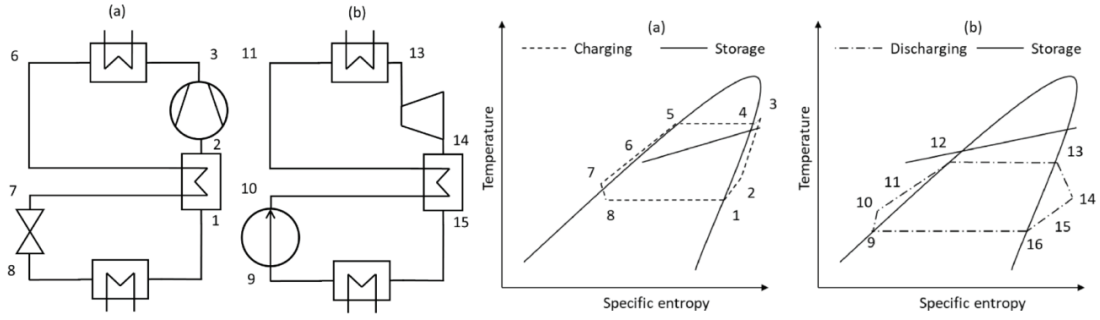

Figure. 1. Heat pump and ORC schematic diagrams (a) and T-s diagrams (b) [9]

3. Thermodynamic modelling

For the study of Carnot Battery systems, the HP/ORC architecture was chosen due to its simplicity and practical feasibility, as well as its low temperatures that facilitate thermal integration; this is also one of the most widely studied types of Carnot Battery, so reference values are readily available.

To study the performance of HP/ORC PTES, each thermodynamic cycle was modelled in MATLAB, with resort to the REFPROP database to calculate fluid properties. Following that, a transient model was developed to simulate the behaviour of a TES coupled to each cycle.

The effectiveness of the Carnot battery process is evaluated through the roundtrip efficiency. The value of this variable is affected by the behaviours of the two sub-cycles of vapor compression heat pump (COP) and the organic Rankine cycle (η), and is expressed by:

$$\varepsilon_{rt} = \mathrm{COP} \times \eta, \tag{1}$$

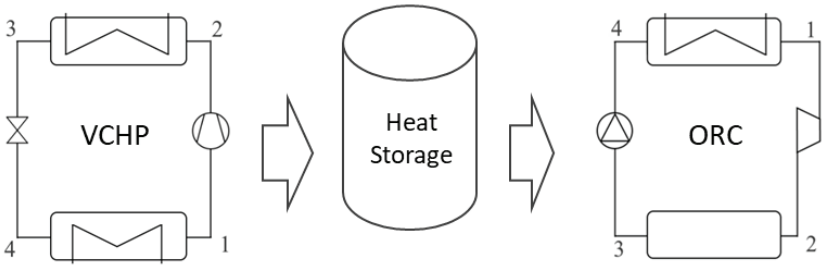

Figure. 2. Schematic representation of the Carnot battery with a simple VCHP, the sensible thermal energy storage and the simple ORC

3.1. Vapor Compression Heat Pump (VCHP)

The standard VCHP cycle is shown in Figure 3 In this cycle, almost all processes involve changes in enthalpy in which case, by definition, heat and/or mechanical work (associated with pressure and volume changes) are being exchanged, neglecting changes in kinetic and potential energy of the fluid.

From points 1 to 2, the enthalpy of the vapour is increased through compression, and the specific work performed on the system is equal to the enthalpy variation:

$$\dot{W}_c = \dot{m}_f(h_2 - h_1), \tag{2}$$

Between 2 and 3, the fluid cools and condenses in a condenser, releasing heat into the HT reservoir at the condensation temperature:

$$\dot{Q}_{cd} = \dot{m}_f(h_2 - h_3), \tag{3}$$

Between 3 and 4, the liquid is expanded into the two-phase region. If this happens in a throttling valve, the process is isenthalpic as heat exchanges can be neglected, and no work is performed on the surroundings. This process is highly irreversible, so it can never be isentropic.

$$h_3 = h_4, \tag{4}$$

Finally, the two-phase mixture receives energy in the evaporator and the fluid returns to a gas state, removing heat from the LT reservoir at the evaporation temperature:

$$\dot{Q}_{ev} = \dot{m}_f(h_1 - h_4), \tag{5}$$

The COP of the heat pump in heating mode is given by the ratio between the heat released from the condenser and the energy consumed in compression. This value is generally greater than unity.

$$COP = \frac{\dot{Q}_{cd}}{\dot{W}_c} \tag{6}$$

In reality, compression may be non-isentropic and there may be superheating of the vapour at point 1, as well as subcooling of the liquid at point 3, in which case the cycle is as shown in Figure 3.2. When the compression process is non-isentropic, which is the case with all real compression processes, the specific entropy of the fluid increases from 1 to 2 – this translates into higher compression work for the non-isentropic process. The isentropic efficiency of a compressor $\eta_{s,c}$ can thus be defined as the ratio between the specific work of the compressor in the isentropic scenario and that of the real scenario:

$$\eta_{s,c} = \frac{w_{c,s}}{w_c} = \frac{(h_{2,s} - h_1)}{(h_2 - h_1)} \tag{7}$$

3.2. Organic Rankine Cycle (ORC)

In the ORC, all processes involve enthalpy changes, as heat and/or mechanical work are exchanged at every step. Between 1 and 2, the vapour is expanded, generating mechanical work – the enthalpy variation is equal to the specific work produced by expansion:

https://doi.org/10.52202/069564-0196

$$\dot{W}_{exp} = \dot{m}_f(h_1 - h_2), \quad (8)$$

From 2 to 3, the working fluid is condensed, rejecting heat to the LT reservoir:

$$\dot{Q}_{cd} = \dot{m}_f(h_2 - h_3), \quad (9)$$

Subsequently, the liquid is pumped to the high-pressure level. The enthalpy variation is equal to the specific work performed by the pump; however, this value is very low as the entire process happens in the liquid phase.

$$\dot{W}_{pump} = \dot{m}_f(h_4 - h_3), \quad (10)$$

Finally, the pressurized liquid is heated and vaporized in the evaporator, drawing heat from the HT reservoir and returning to the state of point 1.

$$\dot{Q}_{ev} = \dot{m}_f(h_1 - h_4), \quad (11)$$

The efficiency of the ORC is given by the ratio between the net energy output, and the heat input at the evaporator:

$$\eta = \frac{\dot{W}_{exp} - \dot{W}_{pump}}{\dot{Q}_{ev}}, \quad (12)$$

As with the vapor compression cycle, the real Rankine cycle involves irreversibilities, some of the most significant being the non-isentropic behavior of the expander and the pump. The isentropic efficiencies of these machines are defined the same way as with the compressor – a ratio between an ideal and a non-ideal amount of work between two states:

$$\eta_{s,exp} = \frac{\dot{W}_{exp}}{\dot{W}_{exp,s}} = \frac{(h_1 - h_{2,s})}{(h_1 - h_{2,s})}, \quad (13)$$

$$\eta_{s,pump} = \frac{\dot{W}_{pump,s}}{\dot{W}_{pump}} = \frac{(h_{4,s} - h_3)}{(h_4 - h_3)}, \quad (14)$$

3.3. Storage Simulation

The TES may use a Sensible Heat Material (SHM), or a Phase Change Material (PCM). PCMs are more energy dense and work well with isothermal processes, however they're often costlier than SHMs [3]. For each case the choice of storage material should be based on several technical, economic, and environmental criteria, a process which is largely outside the scope of this work. Water was chosen as a SHM in the present case, as it presents a high specific heat capacity, low costs and no environmental concerns.

The thermal loss coefficient for the water tank is calculated by the inverse of the sum of a series of thermal resistances corresponding to the thermal barriers that were considered - conduction through a layer of steel and a layer of insulation material, and a convective resistance on the outside of the tank.

$$U_{storage} = \left(R_{cond,steel} + R_{cond,insulation} + R_{conv}\right)^{-1}, \quad (15)$$

The rate of heat loss from the storage to the environment $\dot{Q}$ is determined from the following equation:

$$\dot{Q} = U \cdot A \cdot \Delta T, \quad (16)$$

After the thermodynamic cycles have converged, the energy balance is calculated for the current time step (t) based in the heat transfer rates of charge, discharge and loss to the environment:

$$E_t = E_{t-1} - \left(\dot{Q}_{loss} \times \Delta t\right) + \left(\dot{Q}_{charge} \times \Delta t\right) - \left(\dot{Q}_{discharge} \times \Delta t\right), \quad (17)$$

The updated temperature of the water is obtained, using the equation

$$T_t = \frac{E_t}{m \cdot c_p}, \quad (17)$$

3.4. Dynamic MATLAB model

A dynamic model was developed in MATLAB software which considers the energy content in an insulated cylindrical tank at several points inside a specified time interval, applying an energy balance that considers charge power, discharge power, and losses to the environment.

The cycle begins by considering the first inputs provided by the user, then it proceeds to preliminary simulation of the VCHP and ORC. This determines reference values for mass flow and VCHP/ORC condenser and evaporator power, which are then used to design heat exchange areas for these components in the next step.

After this step, the thermal loss coefficient for the water tank is calculated, its value calculated by the inverse of the sum of a series of thermal resistances corresponding to the thermal barriers that were considered – conduction through a layer of steel and a layer of insulation material, and a convective resistance on the outside of the tank. After this, the iterative cycle begins, each iteration starts by simulating the HP and ORC cycles dynamically, varying the condenser and evaporator temperatures according to the storage tank temperature until the heat exchange rate matches the thermal power associated with phase change. The temperatures of the various points in the thermodynamic cycles, as well as the storage temperature, are constantly updated. The cycle stops when a stopping criterion (for example, a maximum/minimum temperature) is reached, or when it reaches the end of the specified time interval, and then final values are logged and plotted depending on the user's needs. The predefined time interval between two consecutive iterations is 30 seconds but it can be automatically for lower values if a higher resolution is needed, which depends mainly of the thermal energy storage capacity.

The capacity of the storage, nominal power of the compressor and expander, and components' efficiencies are defined inputs of the model as showed in Table 3. The algorithm needs to adjust these input parameters based on the output of the cycle, running the program several times until the desired results are achieved.

4. Results and discussion

4.1. Case study

Using the model presented in Section 3, the case of a solar PV power plant will be analysed. Excess power from the PV array is to be stored as thermal exergy in the water tank and used at night when the solar panels cannot provide any energy. As a means of thermal integration, a solar thermal system is used in conjunction with a secondary hot water tank to boost the temperature of the VCHP evaporator to 70°C. The VCHP compressor receives excess electric energy from the solar PV panels and uses it to upgrade the heat from the evaporator to the required temperature at the condenser. The hot water from the main water tank is then used as a heat source for the ORC, which produces electric energy in the expander as it discharges this heat to the environment. Figure 3 shows the layout of the proposed system.

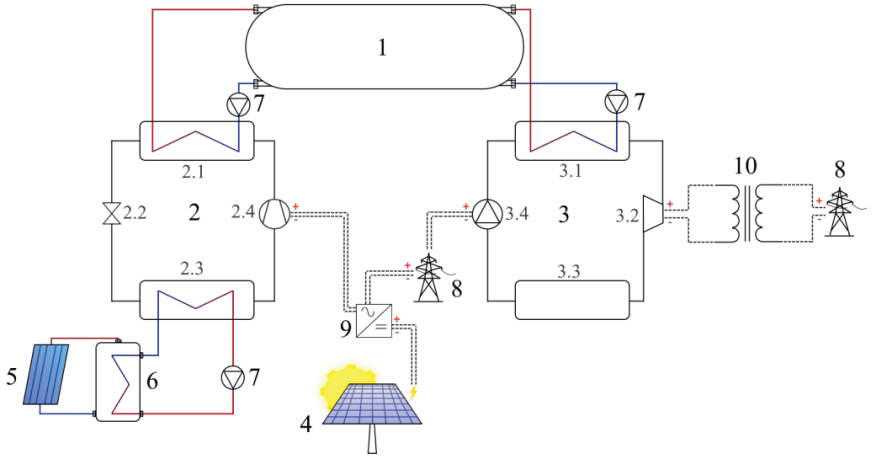

Figure. 3. Schematic representation of the proposed system (1 - Water Tank; 2 - Heat Pump; 2.1 - HP Condenser; 2.2 - HP throttling valve; 2.3 - HP Evaporator; 2.4 - HP Compressor; 3 - ORC; 3.1 - ORC Evaporator; 3.2 - ORC Expander; 3.3 - ORC Condenser; 3.4 - ORC Pump; 4 - PV Array; 5 - Solar thermal panel; 6 - Hot water tank; 7 - Pump; 8 - Power grid; 9 - DC/AC Converter; 10 - AC Transformer).

4.1. Modelling Validation

A first charge/standby/discharge cycle was performed to compare with other studies and obtain initial results and a primary validation, using the values in Table 3. For this first run, a full charge was simulated, followed by 4 hours of standby, and finally a complete discharge of the storage, returning to the initial temperature.

Table 3. *Validation Simulation Parameters.*

Water Tank		**ORC**	
Volume [m^3]	5	Condenser Temperature (design value) [ºC]	35

https://doi.org/10.52202/069564-0196

Aspect Ratio (Length/Diameter)	2	Evaporator Temperature (design value) [ºC]	60
Pressure (Absolute) [bar]	1	Expander Isentropic Efficiency	0.7
Steel Thickness [m]	0.01	Expander Power (design value) [W]	1000
Steel Thermal Conductivity [W/(m.K)]	50	Pump Isentropic Efficiency	0.8
Insulation Thickness [m]	0.05	Subcooling [ºC]	0
Insulation Thermal Conductivity [W/(m.K)]	0.05	Superheating [ºC]	0
VCHP		Evaporator Heat Transfer Coef. (U) [W/(m^2.K)]	1000
Condenser Temperature (design value) [ºC]	100	**Other**	
Evaporator Temperature (design value) [ºC]	60	Ambient Temperature [ºC]	25
Compressor Isentropic Efficiency	0.7	Time Step [s]	30
Compressor Power (design value) [W]	1000	Ambient Convection Coef. [W/(m^2.K)]	10
Subcooling [ºC]	0	Electric Generator Average Efficiency	0.95
Superheating [ºC]	0	Exchangers Pinch Point (design value) [ºC]	10
Condenser Heat Transfer Coef. (U) [ºC]	1000		
Condenser Temperature (design value) [ºC]	100		

The charge phase brought the storage up to a temperature of 90°C in about 17 hours and 46 minutes, with 123.6 kWh of thermal energy variation in the water. With a total electrical consumption of 13.54 kWh, this leads to a global COP of 9.13, factoring in thermal losses to the environment during the charge; if the losses are not considered, the COP is 10.41

The exact values change throughout the charge, as shown in Figure 4. The increase in compressor work and the decrease in condenser thermal power lead to a decrease in the COP as the temperature and pressure in the condenser increase. It can be observed that the VCHP has taken a relatively long time to charge the storage – the charging time mostly depends on the ratio between the total storage heat capacity and the charge power of the heat pump.

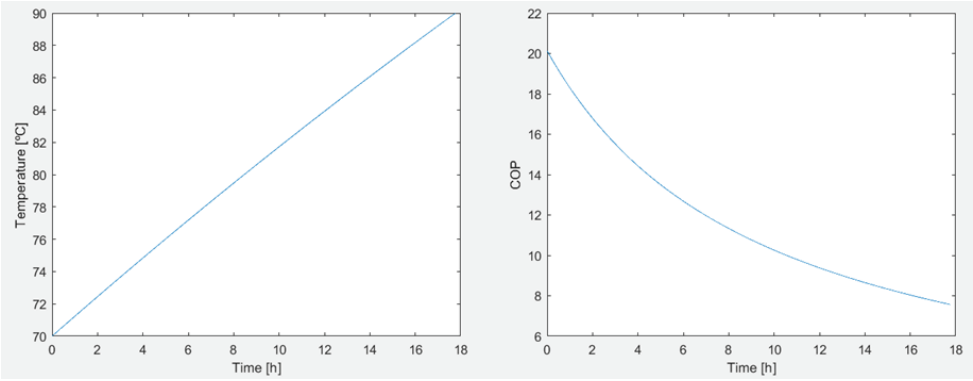

Figure. 4. Evolution of key parameters in the charge phase.

During the standby phase, the temperature of the storage tank decreased slightly due to losses to the environment, with a reduction from 90°C to 89.28°C. This decrease of 0.72°C corresponds to a loss of 4.53 kWh of thermal energy. Figure 5 shows the evolution of the temperature and the thermal loss power from the water tank over the 4-hour period.

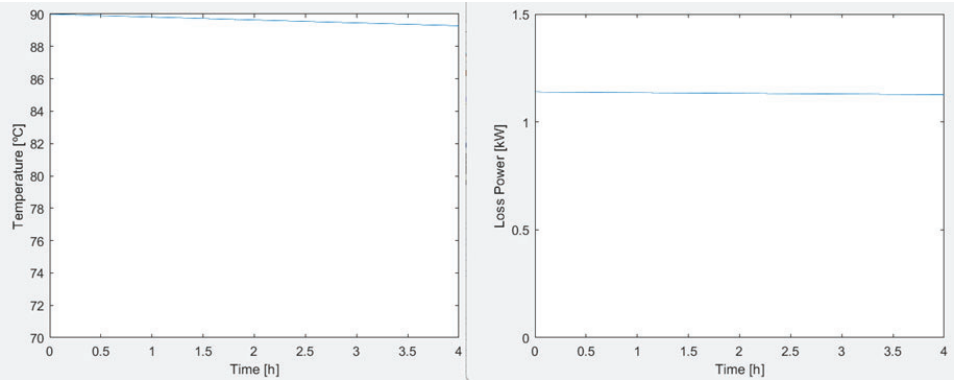

Figure. 5. Evolution of key parameters in the standby phase.

Finally, the discharge phase (Figure 6) brought the storage temperature back down to 70°C in about 10 hours and 27 minutes, with a thermal energy reduction of 119.06 kWh, and a net electrical generation of 8.08 kWh, leading to a global ORC efficiency of 6.8%; factoring out losses to the environment, the global ORC efficiency is 7.4%. With the decrease in evaporator temperature and pressure comes a decrease in evaporator thermal and pump power consumptions, and expander power generation, with an overall decrease in efficiency.

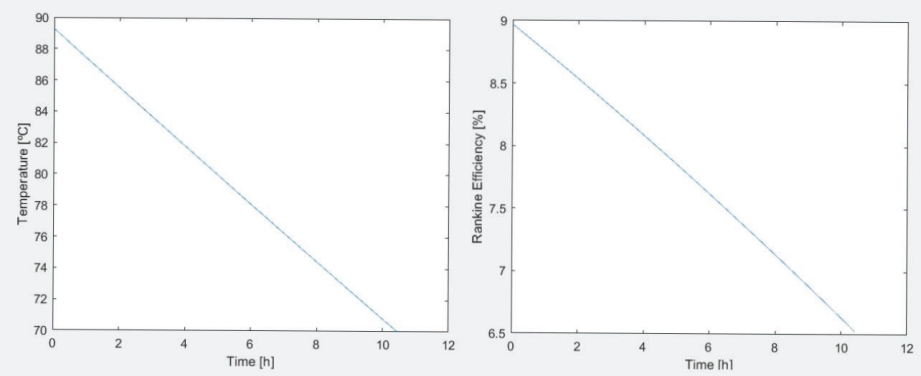

Figure. 6. Evolution of key parameters in the discharge phase.

Roundtrip efficiency is often estimated as the product of the COP with the Rankine efficiency, however this becomes inaccurate when thermal losses from the storage are considered. The use of a dynamic model allows the calculation of a precise value – in this first case, an ε_{rt} of 59.7% was obtained – a value consistent with those obtained in previous studies, and a satisfactory value for a non-optimized situation.

4.2. Optimization Method

The main driving parameters are: expander power, discharge time and charge time. The first two parameters determine an energy requirement, allowing the design of an adequate storage size. The heat pump can then be designed for a power that allows a full charge in 8 hours – roughly the time during which solar energy is available for the PV array.

In terms of optimization, the main objectives are the storage size/temperature variation and heat exchanger surface areas/pinch points. The optimization of these pairs of parameter involves a balance between cost and performance, as the best performance results from the largest surface areas and storage volumes, as these reduce the temperature differences, but they also lead to greater costs. To evaluate the effect of these parameters, a full discharge and a full charge were simulated for five nominal pinch point values (10K, 8K, 6K, 4K, 2K), and five storage temperature spreads at each pinch point (70°C – 75°C, 70°C – 80°C, 70°C – 85°C, 70°C – 90°C and 70°C – 95°C), resulting in a total of 25 charge simulations and 25 discharge simulations. For each case, the storage size was optimized for a 4-hour discharge with a nominal expander power of 20kW, and then a nominal compressor power was chosen to allow a full charge of the storage in 8 hours – these reference powers correspond to the maximum values that will be encountered throughout the simulation.

In terms of costs, the correlations in Table 4 adapted from Santos [10] were used to provide a rough estimate for capital costs in order to make the cost/performance optimization possible. The total cost of the system is given by the sum of the costs for each component.

Table 4. *Cost Correlations for components used in the Carnot Battery.*

https://doi.org/10.52202/069564-0196

Component	Cost Correlation [€]	Unit of Independent Variable
Storage Tank	$2000 + (625 \times Vol._{storage})$	m^3
Heat Exchangers	$150 \times Area$	m^2
ORC Expander	$1.5 \times (225 + (17000 \times \dot{V}_{in}))$	m^3/s
ORC Pump	$900 \times (\dot{W}_{pump}/300)$	W
VCHP Compressor	$225 + (17000 \times \dot{V}_{in})$	m^3/s
Control Electronics	4000	-

4.3. Results

As expected, lower pinch points lead to higher roundtrip efficiency for any storage spread, as this minimizes the temperature gradient of the VCHP and maximizes it for the ORC. A lower storage spread also improves efficiency, as it greatly increases the COP, with only a small decrease in ORC efficiency.

In terms of costs, while the lower pinch points and lower storage spreads lead to higher values (larger heat exchangers and storage tank), the effect of the storage spread seems far greater than that of the pinch point, so the best cost/efficiency ratios are mostly found with the lower pinch points and higher storage spreads – the highest value was obtained for the 10K pinch point and 70°C – 75°C storage spread, at 3979.70 [€/% roundtrip efficiency], with an ε_{rt} of 43.32%. By contrast, the best cost/efficiency ratio was obtained for the 2K pinch point and 70°C – 85°C storage spread, with a value of 586.73 [€/% roundtrip efficiency], and an ε_{rt} of 141.54%. For the 2K pinch point, all storage spreads above 70°C – 75°C return cost/efficiency values below 605 [€/% roundtrip efficiency], with roundtrip efficiencies between 173-105%. At this pinch point, the highest performance is reached with a 70°C – 75°C spread, at a cost/efficiency of 734.37 [€/% roundtrip efficiency], but with an ε_{rt} of 225.54%. In all cases for the 2K pinch point, the system becomes a hybrid between energy storage and a solar thermal power plant, as the efficiency exceeds 100%.

Figure 7 shows how the storage spread (70 – maximum temperature) and pinch point influence the cost/efficiency ratio. It can again be seen that most points along the 2K line are close to the optimal value.

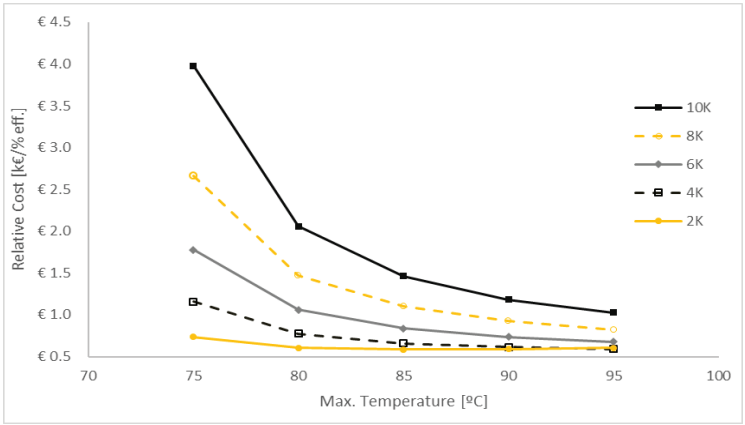

Figure. 7. Maximum storage temperature vs. relative cost for various pinch points.

Finally, payback time was analysed for the various configurations, as shown in Figure 8. The daily profit was calculated as the total electric energy of the discharge phase multiplied by a price of 0.20 €/kWh – a value assumed based on the costs of a few energy providers available in Portugal as well as reference values from the Energy Services Regulatory Authority (ERSE), for a contracted electric power up to 20.7 kVA. Furthermore, the system was assumed to generate this daily profit for 12 months of the year. In reality the performance would generally worsen in the winter months leading to lower profits. Even with enough solar thermal panels to offset unfavourable climate conditions, this fact could potentially affect the payback period in a real situation.

For all storage configurations, the shortest payback times are generally achieved with the 4K, 6K and 8K pinch points, and the shortest payback time between all the simulations is obtained with the 70°C – 95°C spread: approximately 9 years and 2 months. For a payback time of 4 years or lower, the average price of electricity would need to be at least 0.46 €/kWh.

https://doi.org/10.52202/069564-0196

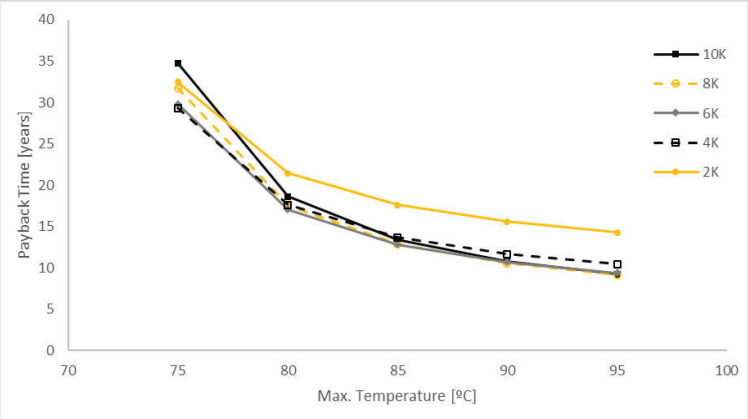

Figure. 8. Maximum storage temperature vs. payback time for various pinch points.

It can be concluded that a select few configurations optimize one parameter or another – the lowest pinch point (2K) and lowest storage spread (70°C – 75°C) optimize performance, the highest pinch point (10K) and the highest spread (70°C – 95°C) optimize costs, the 2K pinch point and 70°C – 85°C spread optimize the cost/performance ratio, and the 8K pinch point and 70°C – 95°C spread optimize the payback period. In this case, all of these solutions are ideal in one form or another – these configurations belong on the so-called Pareto Front (Figure 4.15), the set of all Pareto-optimal solutions. In other words, by moving between the points on this line it is impossible to improve any criterion without deteriorating another. This means that any point on this line represents a valid choice, and the selection should depend on the most relevant priority, or a balance of relevant priorities for a given implementation. For example, from a technological perspective, the best choice is the one with the highest efficiency. In terms of budget alone, the best choice has the lowest cost. For an efficient capital investment, one would select the machine with the best cost/performance ratio, and to minimize the risk of investment the machine with the lowest payback time should be chosen.

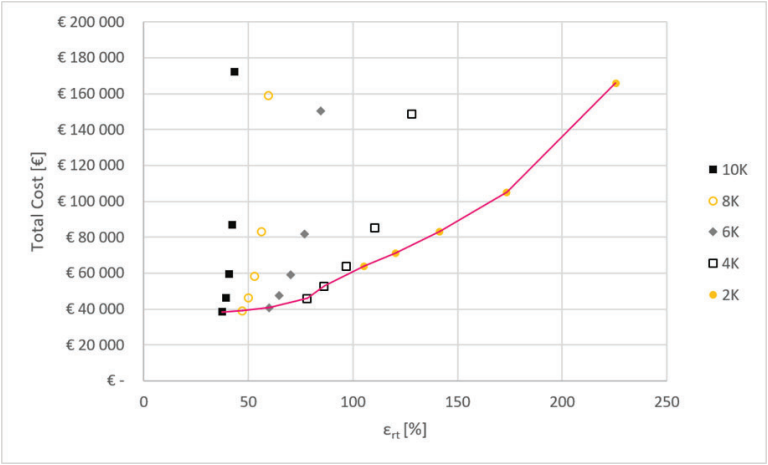

Figure. 9. Pareto Front for the tested configurations.

5. Conclusions

In this study, a case was made for the Carnot Battery as a suitable technology to replace current systems with relatively low Power/Capacity ratios, and a storage duration in the range of a few hours. A MATLAB script was developed which is capable of simulating the performance of a Carnot Battery composed of simple Vapour Compression Heat Pump and ORCs in dynamic charge/discharge conditions, as well as the thermal behaviour of a sensible storage in a standby situation. Despite the limited scope of the present study, the flexibility the developed model should allow its use in diverse situations with little to no modification, including off-design performance, thermal storage material selection, analysis of different thermal integration strategies, as well as more detailed techno-economic studies. Moreover, the model was used to study several configurations, taking into account the most critical parameters of the system, in an effort to discover an optimized arrangement; in the end, the optimal configuration depends on a balance of priorities – if performance is the only criterion, the

https://doi.org/10.52202/069564-0196

lowest pinch point (2K) and lowest storage spread (70°C – 75°C) should be selected despite the high costs; to minimize costs alone, one would select the highest pinch point (10K) and the highest spread (70°C – 95°C) in spite of the low efficiency, and for the best cost/performance ratio, the optimal choice would lie in between these two, with a 2K pinch point and a 70°C – 85°C spread. Additionally, for a minimized payback period the choice would be the 8K pinch point and a 70°C – 95°C spread. It was concluded that these four points belong on the Pareto front, in which all points represent either the optimization of one parameter, or a compromise between multiple parameters, and conclusions were drawn as to the applicability of each configuration.

Acknowledgments

This work is funded by National Funds through the FCT - Fundação para a Ciência e Tecnologia, I.P., under the scope of the project 2022.05282.PTDC.

Nomenclature

A	area, m^2
h	specific enthalpy, kJ/kg
$\dot{m}$	mass flow rate, kg/s
$\dot{Q}$	heat flux, W
R	thermal resistance,
T	temperature, °C
t	time step, s
U	heat transfer coefficient, W/(m^2.K)
$\dot{V}$	volume flow rate, m^3/s
vol	volume, m^3
$\dot{W}$	work, W

Greek symbols

η	efficiency
ε	effectiveness

Subscripts and superscripts

in	inlet
cd	condenser
c	compressor
cond	conduction
conv	convection
ev	evaporator
exp	expander
f	working fluid
loss	thermal loss
pump	flow pump
s	isentropic
rt	roundtrip

References

1. Jafari M, Botterud A, Sakti A. Decarbonizing power systems: A critical review of the role of energy storage. Renewable and Sustainable Energy Reviews. Elsevier Ltd; 2022.

2. Gallo AB, Simões-Moreira JR, Costa HKM, Santos MM, Moutinho dos Santos E. Energy storage in the energy transition context: A technology review. Renewable and Sustainable Energy Reviews. Elsevier Ltd; 2016. p. 800–22.

3. Dumont O, Frate GF, Pillai A, Lecompte S, De paepe M, Lemort V. Carnot battery technology: A state-of-the-art review. J Energy Storage. Elsevier Ltd; 2020;32.

4. Frate GF, Ferrari L, Desideri U. Rankine carnot batteries with the integration of thermal energy sources: A review. Energies (Basel). MDPI AG; 2020.

5. Weitzer M, Müller D, Steger D, Charalampidis A, Karellas S, Karl J. Organic flash cycles in Rankine-based Carnot batteries with large storage temperature spreads. Energy Convers Manag. Elsevier Ltd; 2022;255.

6. Dumont O, Lemort V. Mapping of performance of pumped thermal energy storage (Carnot battery) using waste heat recovery. Energy. Elsevier Ltd; 2020;211.

7. Steinmann WD, Bauer D, Jockenhöfer H, Johnson M. Pumped thermal energy storage (PTES) as smart sector-coupling technology for heat and electricity. Energy. Elsevier Ltd; 2019;183:185–90.

8. Eppinger B, Steger D, Regensburger C, Karl J, Schlücker E, Will S. Carnot battery: Simulation and design of a reversible heat pump-organic Rankine cycle pilot plant. Appl Energy. Elsevier Ltd; 2021;288.

9. Nadeem F, Hussain SMS, Tiwari PK, Goswami AK, Ustun TS. Comparative review of energy storage systems, their roles, and impacts on future power systems. IEEE Access. Institute of Electrical and Electronics Engineers Inc.; 2019. p. 4555–85.

10. Santos M. Modular architecture of steady-state simulation of Rankine based micro combined heat and power systems. 2020; Available from: http://hdl.handle.net/10316/95348